

RADIATIVE TRANSFER IN THE ATMOSPHERE OF MARS AND THAT OF VENUS ABOVE THE CLOUD DECK*

R. D. CESS and V. RAMANATHAN

Department of Mechanics, State University of New York, Stony Brook, N.Y. 11790, U.S.A.

(Received 13 October 1971)

Abstract—The dimensionless parameters which describe radiative transfer within a carbon dioxide atmosphere are shown to yield the same simplifications when applied to the atmospheres of Mars and Venus above the cloud deck. The radiative-transfer formulation correspondingly predicts a middle atmosphere temperature for Mars which is somewhat lower (130°K for the equatorial equinox) than previous theoretical estimates; this result is qualitatively consistent with Mariner 6 and 7 occultation experiments. It is further illustrated that vibrational nonequilibrium is negligible for both Mars and Venus within that portion of the atmospheres where pressure broadening dominates.

Diurnal changes in the atmospheric temperature profile for Venus, which result from the time dependence of solar heating, are also considered. It is shown that there exists a region above the cloud deck, exceeding 20 km in height, within which atmospheric temperature is independent of time. This is in qualitative agreement with the Mariner 5 occultation experiments. In the middle atmosphere, assuming a four-day rotation for this portion of the atmosphere, a diurnal temperature variation of 33°K is predicted.

1. INTRODUCTION

ANALYSES involving radiative transfer in the Martian atmosphere have been presented by PRABHAKARA and HOGAN,⁽¹⁾ OHRING and MARIANO,^(2,3) and GIERASCH and GOODY,^(4,5) while a radiative equilibrium analysis for the atmosphere of Venus has been performed by BARTKO and HANEL.⁽⁶⁾ From the viewpoint of radiative transfer, the atmospheres of Mars and Venus bear obvious similarities, since it is now well known that the major constituent of both atmospheres is carbon dioxide. The lower atmosphere of Venus, however, possesses a cloud cover of unknown composition. Furthermore, above the cloud tops there is evidence of less dense clouds or haze, whose contribution to atmospheric radiation is again not known. To a first approximation, however, it would appear reasonable to assume that radiative transfer within the atmosphere of Venus above the clouds is due solely to carbon dioxide. Consequently, there exists the possibility of developing a unified treatment for radiative transfer in the atmosphere of Mars and that of Venus above the cloud deck.

In the present investigation, particular emphasis will be placed upon the dimensionless parameters which describe the radiative transfer process and the simplifications which result from the magnitudes of these parameters. Specifically, it will be shown that the same simplifications are appropriate for both Mars and Venus. Following an illustrative radiative

* This research was supported by the National Science Foundation through Grant No. GK-16755.

equilibrium solution, the radiative transfer formulation is employed to study diurnal variations in the atmospheric temperature profile for Venus.

2. RADIATIVE FLUX EQUATION

For the present purposes, attention will be directed towards that portion of the atmosphere for which pressure broadening (as opposed to Doppler broadening) may be assumed. As indicated by Gierasch and Goody,⁽⁴⁾ this is reasonable for the lower 35 km of the Martian atmosphere, while an extrapolation to Venus indicates a region extending approximately 40 km above the cloud deck. The height of the cloud deck is roughly 57 km.⁽⁷⁾

Infrared transmission within a carbon dioxide atmosphere is due primarily to the 15μ fundamental band, while solar absorption results from the near infrared bands.⁽⁴⁾ The radiative energy flux is in turn described in terms of the total band absorptance, such that, for example, extending equation (4) of CESS⁽⁸⁾ to a multiple band spectra, the radiative flux q_R may be expressed as

$$q_R = \sigma T_g^4 - \mu\alpha\sigma T_s^4 - \int_0^{u_{01}} \frac{de_{\omega 1}}{du'} A(|u_1 - u'|) du' - e_{\omega 1}(0)A(u_1) + \mu\alpha \sum_{i=2}^N e_{\omega i}(T_s)A(u_i/\mu), \quad (1)$$

where

$$u_i = \frac{3S_i}{2A_{0i}} \int_y^\infty P dy \quad (2)$$

with A_{0i} denoting the bandwidth parameter⁽⁹⁾ and S_i the band intensity, while P is pressure and y the vertical coordinate measured from the surface (or cloud top). The subscript i refers to the specific band, with $i = 1$ denoting the 15μ band, whereas $i \geq 2$ refer to the near infrared solar absorption bands, and N represents the total number of bands. Furthermore, $\sigma =$ Stefan-Boltzmann constant, $T_g =$ surface temperature (or cloud top temperature for Venus), $T_s =$ effective black-body temperature of the sun, $\mu = \cos \theta$, where θ is the solar zenith angle, $A(u_i) =$ total band absorptance, $\omega =$ wave number, $e_{\omega i} =$ Planck's function at the center of band i , $e_{\omega 1}(0) =$ Planck's function at temperature corresponding to $u_1 = 0$, $\alpha = (R_s/L)^2$, where R_s is the radius of the sun and L the distance between the planet and the sun, $u_{0i} = u_i$ at $y = 0$. Note that u_i represents a dimensionless coordinate measured from the top of the atmosphere. In addition, for an atmosphere in hydrostatic equilibrium such that $P(y) = P(0) \exp(-y/H)$, it readily follows that $u_{0i} = 3S_i H P(0) / 2A_{0i}$, where H is the atmospheric scale height.

3. BAND ABSORPTANCE FORMULATION

In order to apply equation (1) to a carbon dioxide atmosphere, it is first necessary to have available a formulation for the total band absorptance of the important vibration-rotation bands. This may be expressed in terms of two parameters, one of which is the dimensionless scaled amount, u_i , as defined by equation (2). The factor $3/2$ results from

assuming a mean atmospheric slant path in accordance with the exponential kernel approximation.⁽⁸⁾ The second required parameter is the line-structure parameter. Employing the Curtis–Godson approximation,^(3,4) the appropriate scaled parameter is

$$\beta = 2\gamma_0 P(0)u_j/du_{0i}, \quad (3)$$

where γ_0 is the mean rotational line width per unit pressure, and d is the mean line spacing. Assuming γ_0/d to be the same for all bands, β is found to be independent of band specification.

The mean rotational line width for self-broadening of CO₂ has been evaluated from the rotational line-width calculations of YAMAMOTO *et al.*⁽¹⁰⁾ in accordance with the relation⁽¹¹⁾

$$\sqrt{\gamma_0} = \frac{\sum_{j=0}^{\infty} \sqrt{(\gamma_{0j} S_j)}}{\sum_{j=0}^{\infty} \sqrt{S_j}}, \quad (4)$$

where j is the rotational quantum number. This average is appropriate to the square-root limit, for which line structure is of maximum importance. It was found that the numerical results for $\gamma_0(T)$ could be represented by

$$\gamma_0(T) = 0.097 \left(\frac{300}{T} \right)^{2/3} \text{ cm}^{-1} \text{ atm}^{-1}. \quad (5)$$

Equation (5) is applicable for the temperature levels of present interest. At higher temperatures, an additional averaging over vibrational quantum number is necessary.^(12,13) The mean line spacing, for alternate lines missing, was taken to be $d = 4B$, where B is the rotational constant.

In terms of the scaled parameters u and β , the band absorptance should satisfy the following three limits:^(9,11) $A = A_0 u$ for $u \ll 1$; $A = 2A_0 \sqrt{\beta u}$ for $\beta \ll 1$, $u/\beta \gg 1$, $\beta u \ll 1$; $A = A_0 \ln u$ for $u \gg 1$. A further constraint⁽¹¹⁾ is that the linear and logarithmic limits must be achieved irrespective of whether or not one first imposes the overlapped line limit ($\beta = \infty$). A number of band absorptance correlations are available,^(9,11,14,15) and a particularly simple one which satisfies all of these conditions is⁽¹¹⁾

$$A(u) = 2A_0 \ln \left\{ 1 + \frac{u}{2 + \sqrt{u(1 + 1/\beta)}} \right\}. \quad (6)$$

Choosing a mean atmospheric temperature of 180°K for both Mars and Venus, taking $P(0) = 0.005$ atm and $H = 9.2 \times 10^5$ cm for Mars, while $P(0) = 0.3$ atm and $H = 4.7 \times 10^5$ cm for Venus, and employing⁽¹⁶⁾ $A_{01} = 17.3 \text{ cm}^{-1}$ and⁽¹⁷⁾ $S_1 = 549 \text{ atm}^{-1} \text{ cm}^{-2}$, maximum values of the band parameters for the 15 μ band are illustrated in Table 1. For both atmospheres, $\beta \ll 1$ while $u/\beta \gg 1$ so that equation (6) reduces to

$$A(u) = 2A_0 \ln[1 + \sqrt{\beta u}]. \quad (7)$$

This simplification is also valid for the important near infrared bands. Equation (7) is similar to the expression employed by GIERASCH and GOODY⁽⁴⁾ for the 15 μ band, although it has been obtained by a somewhat different means.

TABLE 1. BAND PARAMETERS FOR THE 15 μ CARBON DIOXIDE BAND

	Mars	Venus
$\beta \leq$	8.7×10^{-4}	5.3×10^{-2}
$u_1 \leq$	2.2×10^5	6.7×10^6
$\beta u_1 \leq$	1.9×10^2	3.5×10^5
$u_1/\beta =$	2.5×10^8	1.3×10^8

The condition $u_1/\beta \gg 1$ implies the strong-line limit and equation (7) constitutes a transition from the square-root ($\beta u \ll 1$) to the logarithmic ($\beta u \gg 1$) limits. Note that the linear limit is not achieved for $u \rightarrow 0$. However, since $\beta \sim u$, the square-root limit for a nonhomogeneous atmosphere is mathematically analogous, although physically quite different, to the linear limit for a homogeneous gas.

Employing equations (1) and (7), one may now proceed to formulate the divergence of the radiative flux vector with the result that

$$\frac{1}{A_{01}e_{\omega_1}(T_g)} \frac{dq_R}{d\xi} = - \int_0^{\xi} \frac{d\phi}{d\xi'} \frac{d\xi'}{[1 + \sqrt{(\xi - \xi')}] \sqrt{(\xi - \xi')}} - \frac{\phi(0)}{\sqrt{(\xi) + \xi}} + \int_{\xi}^{\xi_0} \frac{d\phi}{d\xi'} \frac{d\xi'}{[1 + \sqrt{(\xi' - \xi)] \sqrt{(\xi' - \xi)}}} + \sum_{i=2}^N \frac{\Gamma_i}{\sqrt{(\xi/\bar{\mu}_i) + \xi/\bar{\mu}_i}}, \quad (8)$$

where

$$\phi = \frac{e_{\omega_1}(T)}{e_{\omega_1}(T_g)}, \quad \xi = \beta u_1, \quad \xi_0 = \beta_0 u_{01}, \quad \bar{\mu}_i = \frac{3\mu S_1 A_{0i}}{2S_i A_{01}}, \quad \Gamma_i = \frac{2\alpha S_i e_{\omega_i}(T_s)}{3S_1 e_{\omega_1}(T_g)},$$

β_0 denotes the maximum value of β . The only basic difference between equation (8) and that of GIERASCH and GOODY⁽⁴⁾ for the Martian atmosphere lies in the formulation of the solar absorption term.

With reference to Table 1, it is apparent that $\xi_0 \gg 1$; this condition greatly facilitates the application of equation (8) to a specific energy-transfer problem. In the following, two cases will be considered. The first is a solution for radiative equilibrium, which will be presented solely for the purpose of illustrating certain basic features of the radiative-transfer process. The second case involves the physically more meaningful analysis of the time-dependent diurnal variation of the atmospheric thermal structure for Venus.

4. RADIATIVE EQUILIBRIUM

The state of radiative equilibrium is described by $dq_R/d\xi = 0$. The integral equation defining $\phi(\xi)$ follows now directly from equation (8). The asymptotic solution of this equation for $\xi_0 \gg 1$ is obtained in a manner similar to that discussed by CESS,⁽⁸⁾ with the result that

$$\phi(\xi) = 1 + \frac{C\pi}{2} + C \sin^{-1} \left(1 - 2 \frac{\xi}{\xi_0} \right). \quad (9)$$

The constant C arises from the fact that the asymptotic form of the integral equation does not possess a unique solution. It may further be shown⁽⁸⁾ that equation (9) does not apply in the vicinity of $\xi = 0$. Equation (9) thus constitutes what will be termed a lower solution, while the appropriate upper solution (or middle atmosphere solution) is found from equation (8) to be

$$\phi(0) = \sum_{i=2}^N \Gamma_i \sqrt{\bar{\mu}_i}. \quad (10)$$

The constant C is thus determined by matching equations (9) and (10); this procedure is simply a matched asymptotic expansion or singular perturbation.⁽¹⁸⁾ The result is

$$C = -\frac{1}{\pi} \left[1 - \sum_{i=2}^N \Gamma_i \sqrt{\bar{\mu}_i} \right] \quad (11)$$

such that equations (9) and (11) completely define $\phi(\xi)$.

Physically, the upper solution corresponds to the isothermal portion of the atmosphere. For a homogeneous gas, this result would denote the linear (or optically thin) limit and recall the previous discussion pertaining to the mathematical analogy between the non-homogeneous atmosphere for $u \rightarrow 0$ and the linear limit for a homogeneous gas.

Since equations (9) and (11) constitute an asymptotic solution for $\xi_0 \gg 1$, ξ_0 does not appear as a separate parameter in the solution. The radiative equilibrium temperature profile is thus independent of both the line structure parameter β_0 and the dimensionless amount u_{01} . This conclusion is consistent with the numerical findings of GIERASCH and GOODY.⁽⁴⁾ It is of further interest to note that this independence on $\xi_0 \gg 1$ is quite analogous to the invariance of the temperature profile with pressure for a homogeneous gas with $u_0 \gg 1$. This result has been predicted theoretically by EDWARDS *et al.*,⁽¹⁶⁾ and by CESS and TIWARI,⁽¹⁹⁾ it has recently been observed experimentally by SCHIMMEL *et al.*⁽²⁰⁾

In order to rephrase $\phi(\xi)$ as $T(y/H)$ for a carbon dioxide atmosphere, bandwidth parameters have been taken from EDWARDS *et al.*,⁽¹⁶⁾ while the band intensities are from the summary by TIEN.⁽¹⁷⁾ These are listed in Table 2, with only the 4.3 and 2.7 μ bands being included for solar absorption. It will shortly be shown that the additional near-infrared bands produce a negligible contribution to solar absorption.

TABLE 2. BAND CORRELATION PARAMETERS FOR CARBON DIOXIDE AT 180°K

i	ω_i, cm^{-1}	A_{0i}, cm^{-1}	$S_i, \text{atm}^{-1} \text{cm}^{-2}$
1	667	17.3	549
2	2350	15.4	4505
3	3715	32.2	102

Taking $T_s = 5785^\circ\text{K}$ and employing Wien's approximation of Planck's function for $e_{\omega_1}(T)$, it follows that

$$\phi(0) = \sum_{i=2}^3 \Gamma_i \sqrt{\bar{\mu}_i} = 176\alpha \sqrt{\mu} \exp(960/T_s), \quad (12)$$

while T and ϕ are related by

$$\frac{960}{T} = \frac{960}{T_g} - \ln \phi. \quad (13)$$

Again employing $P(y) = P(0) \exp(-y/H)$, we find

$$\frac{y}{H} = \frac{1}{2} \ln(\xi_0/\xi). \quad (14)$$

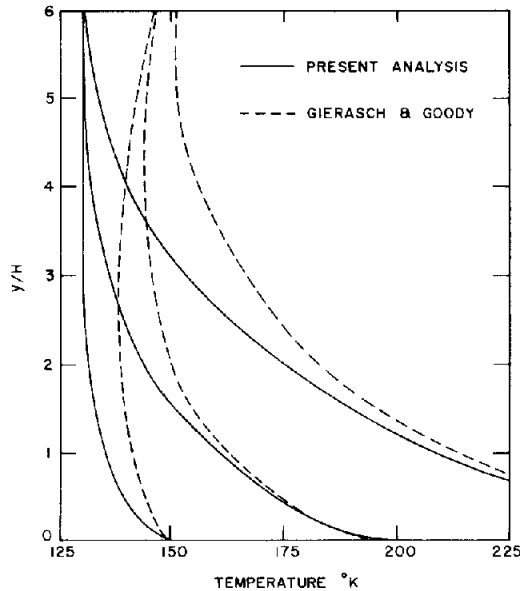


FIG. 1. Comparison of results for radiative equilibrium in the atmosphere of Mars with $\mu = 0.5$.

A comparison of the present analysis with the radiative equilibrium results of GIERASCH and GOODY⁽⁴⁾ is illustrated in Fig. 1 for several assumed surface temperatures. Both solutions are for $\mu = 0.5$, while α in equation (12) is replaced by $\alpha/2$ to give an average solar irradiation, with $\alpha = 0.932 \times 10^{-5}$ for Mars.* Figure 1 shows that the trends of the two solutions are quite similar, although the present results yield the somewhat lower middle atmosphere temperature of 129°K. This is interesting in the light of the Mariner 6 and 7 occultation experiments,^(21,22) which indicate lower atmospheric temperatures for Mars than previously anticipated. An independent calculation of the middle atmosphere temperature has further been performed employing the band absorptance correlation of HOUGHTON.⁽²³⁾ This yielded 134°K considering only the 4.3 and 2.7 μ bands for solar absorption, while inclusion of three additional bands in the 2.0–1.4 μ range increased the temperature by less than 1°K. A further discussion of the middle atmosphere temperature for Mars is given in the next section.

* The present method of calculating the incident solar radiation gives values which are virtually identical with those employed by OHRING and MARIANO.⁽¹³⁾

To assess the accuracy of the asymptotic solution for $\xi_0 \gg 1$, together with the simplifications employed in going from equation (6)–(7), a numerical solution for radiative equilibrium in the Martian atmosphere was performed. The numerical and asymptotic solutions were found to agree to within four significant figures.

The present solution has particular utility with respect to the possible occurrence of vibrational nonequilibrium. Conventionally, departures from local thermodynamic equilibrium are assumed to take place when the ratio η/η_r is not small, where η is the vibrational relaxation time and η_r the radiative lifetime. With reference to the middle atmospheres of Mars and Venus, the value of η/η_r could be of the order of unity. This ratio, however, does not constitute the sole indication of non-LTE. For example, letting $\phi^*(0)$ denote a dimensionless non-LTE source function for the middle atmosphere, then, following GIERASCH and GOODY⁽⁴⁾ and TIWARI and CESS,⁽²⁴⁾ this is related to the LTE function $\phi(0)$ by

$$\phi^*(0) = \phi(0) \left[1 - \frac{3}{4} \left(\frac{\eta}{\eta_r} \right) \sqrt{\left(\frac{\beta_0}{u_{01}} \right)} \right].$$

With reference to Table 1, $\sqrt{\beta_0/u_{01}}$ is of $O(10^{-4})$ for Mars and Venus. This result clearly illustrates that departures from LTE are of no significance for that portion of either atmosphere within which pressure broadening dominates.

As illustrated by GIERASCH and GOODY,⁽⁵⁾ the assumption of radiative equilibrium is totally invalid for the lower region of the Martian atmosphere. The sole intent of the present section has been to examine certain features of the radiative-transfer process. In the following section, consideration is given to diurnal changes in the atmospheric temperature profile resulting from time-dependent solar heating. The primary application will be to the atmosphere of Venus, although brief consideration will be given to the middle atmosphere of Mars.

5. DIURNAL ANALYSIS

Since the cloud-top temperature for Venus is essentially independent of local time, diurnal changes in the thermal structure of the atmosphere above the cloud deck are due solely to the time dependence of solar heating. The rotation rate of Venus is very slow (a solar day on Venus is roughly 117 Earth days), and it has been customary to assume that the atmosphere responds instantaneously to changes in solar heating, i.e. the quasi-steady assumption is made for which the unsteady term in the energy equation is deleted (e.g. BARTKO and HANEL⁽⁶⁾).

To assess this assumption in more quantitative terms, consider the unsteady energy equation

$$\rho C_p \frac{\partial T}{\partial t} = - \frac{\partial q_R}{\partial y}, \quad (15)$$

where t denotes time, while ρ and C_p are density and specific heat, respectively. Further,*

$$\mu = \cos \Theta \cos \Omega t, \quad (16)$$

* For Mars, this relation applies only at the equinox.

where Ω is the rotational velocity of the planet, Θ is latitude, and t is measured from local noon. For illustrative purposes, we write

$$\frac{\partial T}{\partial t} = \frac{\partial e_{\omega_1}}{\partial t} \frac{dT}{de_{\omega_1}} \tag{17}$$

and, employing the previously specified nomenclature, equation (15) may be recast as

$$\varepsilon \frac{\partial \phi}{\partial \tau} = \frac{\xi^{1/2}}{A_{01} e_{\omega_1}(T_g)} \frac{\partial q_R}{\partial \xi}, \tag{18}$$

where $\tau = \Omega t$ while

$$\varepsilon = \left(\frac{C_p \Omega}{3S_1 TR} \right) \sqrt{\left(\frac{u_{01}}{\beta_0} \right) \left(\frac{dT}{de_{\omega_1}} \right)} \tag{19}$$

with R denoting the gas constant.

The procedure for dealing with equation (18) follows that of the previous section for radiative equilibrium. Considering first the upper region (middle atmosphere), letting Φ denote ϕ within this region, and evaluating $\xi^{1/2}(\partial q_R/\partial \xi)$ from equation (8) with $\xi \rightarrow 0$, the unsteady energy equation for the middle atmosphere becomes

$$\varepsilon \frac{d\Phi}{d\tau} + \Phi = HF(\tau), \tag{20}$$

where

$$H = 176\alpha e^{960/T_g} \sqrt{(\cos \Theta)},$$

while

$$F(\tau) = \begin{cases} \sqrt{(\cos \tau)} & \text{for } \cos \tau > 0, \\ 0 & \text{for } \cos \tau < 0. \end{cases}$$

Although T_g appears in the expression for H , the middle atmosphere temperature is actually independent of T_g since a cancelling term is present in equation (13). A similar conclusion follows from the diurnal analysis of GIERASCH and GOODY⁽⁵⁾ for Mars.

Basically, the parameter ε may be regarded as the ratio of the middle atmosphere response time to the rotation time. Equation (20) is applicable to both Mars and Venus. It is now of interest to digress briefly to Mars for which $\Omega = 0.71 \times 10^{-4} \text{ sec}^{-1}$, giving $\varepsilon = 12$. This relatively large value for ε would imply that the middle atmosphere of Mars does not respond to diurnal changes in solar absorption. Indeed, since the unsteady term in equation (20) is at most of $\mathcal{O}(\Phi)$ then, for $\varepsilon \gg 1$, it follows that $d\Phi/d\tau$ must be small. This conclusion is in agreement with the diurnal analysis of GIERASCH and GOODY.⁽⁵⁾

Since the middle-atmosphere temperature is essentially independent of time, it may be evaluated by averaging equation (20) over a solar day and letting $\bar{\Phi}$ denote this average; then

$$\bar{\Phi} = \frac{H}{2\pi} \int_0^{2\pi} F(\tau) d\tau = 0.382H. \tag{21}$$

For Mars, $\alpha = 0.932 \times 10^{-5}$ and, at the equatorial equinox, this gives a middle-atmosphere temperature of 130 as compared to 153°K from the diurnal analysis of GIERASCH and GOODY.⁽⁵⁾

Returning now to Venus for which $\Omega = 6.2 \times 10^{-7} \text{ sec}^{-1}$, based on a solar day, one finds that $\epsilon = 0.054$. Although this result indicates that the response time is very small compared to the rotation time, it does not imply that the quasi-steady assumption is valid. With reference to equation (20), it is obvious from the solution for $\epsilon = 0$ that $d\Phi/d\tau$ is singular at sunset and sunrise. Thus, even though $\epsilon \ll 1$, the unsteady term must still be important during certain time intervals. The upper solution has consequently been evaluated with the unsteady term retained. This objective was accomplished by numerically integrating the nonlinear counterpart to equation (20), i.e. the form of the energy equation for which equation (17) has not been employed. The solution is illustrated by the $\epsilon = 0.054$ curve in Fig. 2.

A comparison of the numerical solution with the quasi-steady solution is shown in Fig. 2 for $\Theta = 0$. The quasi-steady assumption is valid in the vicinity of noon ($\tau = 0$) but, as expected, a significant departure occurs at sunset ($\tau = \pi/2$). During the night, the quasi-steady assumption predicts a zero temperature upper region due to the lack of solar absorption, while the unsteady solution illustrates a rather slow transient cooling process until sunrise ($\tau = 3\pi/2$).

There are two caveats which must be imposed upon the results of Fig. 2. One concerns the possibility of condensation of carbon dioxide, with a subsequent influence upon

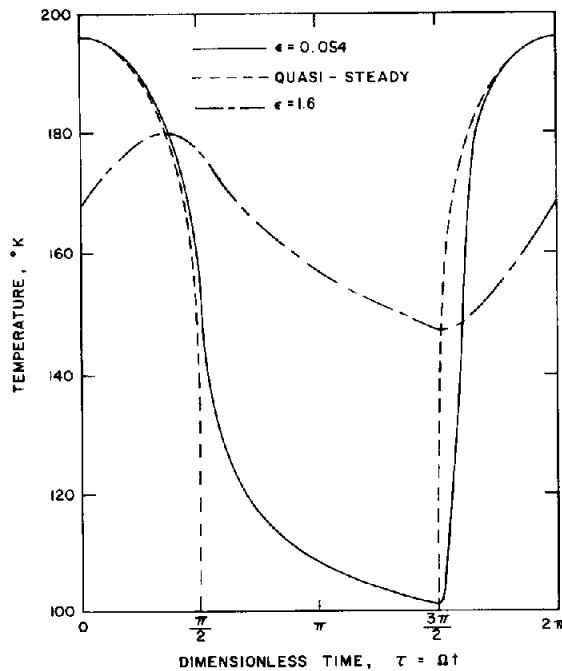


FIG. 2. Comparison of results for the diurnal variation of the middle atmosphere temperature of Venus at the equator.

atmospheric temperature, due to the low temperatures predicted during the night. The likelihood of condensation may, however, be modified by the second factor, which is the four-day retrograde rotation in the Venus atmosphere. U.V. photographs^(2.5-2.7) indicate strong winds (roughly 100 m/sec) acting in the same direction as the planet's rotation. The altitude of these observations is in the vicinity of 10 km above the visible clouds. Winds of this magnitude have also been postulated in the upper atmosphere as a basis for explaining the Mariner 5 measurements of ion^(2.8) and oxygen atom^(2.9) densities. It appears that the entire middle and upper atmosphere might rotate as a coherent shell with a four-day rotation.

It has been suggested that this atmospheric rotation is driven by periodic thermal forcing. GIERASCH,^(3.0) for example, has employed an approximation to the quasi-steady results of BARTKO and HANEL⁽⁶⁾ to estimate thermally driven winds, and he finds large wind velocities acting in the correct direction. GOLD and SOTER,^(3.1) on the other hand, propose that the winds are produced through a solar couple upon a thermal semidiurnal atmospheric tide.

Regardless of the forcing mechanism, the winds would certainly reduce the magnitude of the diurnal temperature variation. The results of GIERASCH,^(3.0) for example, indicate that the magnitude of the diurnal thermal oscillation is reduced by roughly an order of magnitude. To explore this further within the framework of the present analysis, it will be assumed that the middle atmosphere undergoes a solid-body four-day rotation. Since the lower atmosphere does not influence the temperature of the middle atmosphere, then the modification of equation (20) simply involves multiplying ε by 117/4, which is the ratio of the planetary solar day to that assumed for the middle atmosphere. This yields $\varepsilon = 1.6$, implying comparable rotation and response times for the middle atmosphere.

The nonlinear counterpart of equation (20) has been numerically integrated for $\varepsilon = 1.6$ and the resulting diurnal variation of the middle atmosphere temperature is included in Fig. 2. The amplitude of the diurnal variation is reduced by roughly a factor of three compared to the temperature variation for which the middle atmosphere is assumed to rotate with the planet. The higher temperatures occurring during the night probably preclude the possibility of carbon dioxide condensation. Note also that the peak temperature lags the time of maximum solar heating by about $\pi/3$. A comparable lag has been predicted by GIERASCH.^(3.0)

With reference to the lower region, employing the asymptotic form of equation (8) for $\xi_0 \gg 1$ ⁽⁸⁾ and combining this with equation (18), the unsteady energy equation for the lower atmosphere becomes

$$\tilde{\varepsilon} \frac{\partial \phi}{\partial \tau} = \sqrt{\zeta} \int_0^1 \frac{\partial \phi}{\partial \zeta'} \frac{d\zeta'}{\zeta' - \zeta}, \quad (22)$$

where $\zeta = \xi/\xi_0$ and $\tilde{\varepsilon} = \varepsilon\sqrt{(\beta_0 u_{01})}$. The quantity $\tilde{\varepsilon}$ simply denotes the ratio of response to rotation times for the lower atmosphere. Considering the solar day to be that of the planet ($\varepsilon = 0.054$), then $\tilde{\varepsilon} = 31$. This yields the rather surprising result that the lower atmosphere will not respond to diurnal changes imposed upon it by the upper region. Evidently this implies that one must include either a separate transition solution or a more sophisticated asymptotic matching than was necessary in the previous radiative equilibrium example. This has not yet been attempted.

In any event, however, it is now possible to postulate a qualitative diurnal model for the atmosphere of Venus above the cloud deck, and this is illustrated in Fig. 3. The main point is that there should exist a region for which the temperature profile is independent of time.

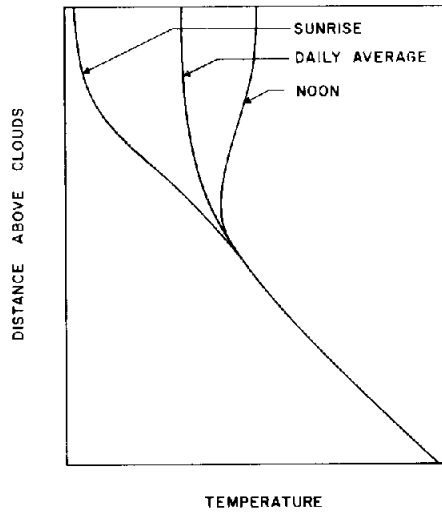


FIG. 3. Proposed diurnal thermal structure for the atmosphere of Venus above the cloud deck.

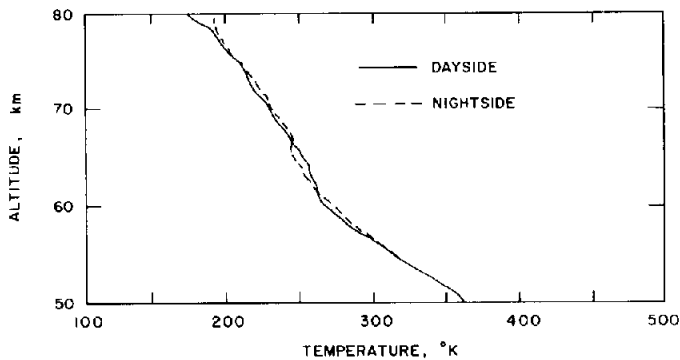


FIG. 4. Atmospheric temperature profiles for Venus from the Mariner 5 occultation experiments as reported by Fjeldbo, Kliore and Eshleman.⁽³²⁾

Figure 4 shows a comparison of the dayside and nightside temperature profiles obtained from the Mariner 5 occultation experiments reported by FJELDBO *et al.*⁽³²⁾ The dayside profile corresponds roughly to noon and a latitude of 30°S, as opposed to midnight and 30°N for the night-side profile. Below 60 km (which is approximately the postulated cloud top location) the lapse rate is adiabatic, indicating a convective region. Above 60 km a subadiabatic lapse rate exists, and this implies the absence of significant vertical convection.

It should be cautioned, however, that other interpretations involving water vapor condensation and ice sublimation are possible.^(3,2) If these processes are not important, then it is the region above 60 km which corresponds to the proposed structure of Fig. 3. The interesting feature is that there is essentially no difference between the dayside and nightside profiles, and this is in agreement with the lower portion of Fig. 3. Unfortunately, the occultation data do not apply to higher altitudes to indicate whether or not a transition to an unsteady region occurs.

There are two further statements that may be made concerning comparison of the present qualitative results with the profiles of Fig. 4. The first involves the temperature to which the lower region profile should asymptotically approach. Although a time-averaged middle atmosphere temperature has little meaning, it does constitute the asymptotic limit for the lower solution, since the lower region temperature is independent of time. Employing equation (21) with $\Theta = 30^\circ$ and $\alpha = 4.23 \times 10^{-5}$ for Venus, one obtains 162°K, with reference to Fig. 4 this would not be an unreasonable asymptotic limit for the observed profiles.

The second point is whether or not the altitude range in Fig. 4 is actually indicative of that portion of the atmosphere for which equation (22) is applicable. In other words, is the 80 km altitude within the lower region? To investigate this, note that the right hand side of equation (22) follows from equation (8) with $\xi \gg 1$, such that the lower region corresponds to that portion of the atmosphere for which $\xi \gg 1$. Furthermore, ξ is a coordinate measured from the top of the atmosphere, and the 80 km altitude corresponds to $\xi \simeq 70$. Thus, the portion of the atmosphere depicted by Fig. 4 is certainly within the lower region.

Acknowledgement—The authors are indebted to Mr. V. KAPUR for performing the numerical computations.

REFERENCES

1. C. PRABHAKARA and J. S. HOGAN, JR., *J. Atmos. Sci.* **22**, 97 (1965).
2. G. OHRING and J. MARIANO, *J. Atmos. Sci.* **23**, 251 (1966).
3. G. OHRING and J. MARIANO, *J. Atmos. Sci.* **25**, 673 (1968).
4. P. GIERASCH and R. GOODY, *Planet. Space Sci.* **15**, 1465 (1967).
5. P. GIERASCH and R. GOODY, *Planet. Space Sci.* **16**, 615 (1968).
6. F. BARTKO and R. A. HANEL, *Astrophys. J.* **151**, 365 (1968).
7. D. M. HUNTEN and R. M. GOODY, *Science* **165**, 1317 (1969).
8. R. D. CESS, *JQSRT* **11**, 1699 (1971).
9. D. K. EDWARDS and W. A. MENARD, *Appl. Optics* **3**, 621 (1964).
10. G. YAMAMOTO, M. TANAKA and T. AOKI, *JQSRT* **9**, 371 (1969).
11. R. D. CESS and S. N. TIWARI, Infrared Radiative Energy Transfer in Gases, *Advances in Heat Transfer*, Vol. 8. Academic Press, New York (in press).
12. D. K. EDWARDS, *Appl. Opt.* **4**, 1352 (1965).
13. D. K. EDWARDS and W. A. MENARD, *Appl. Opt.* **3**, 847 (1964).
14. C. L. TIEN and J. E. LOWDER, *Int. J. Heat Mass Transfer* **9**, 698 (1966).
15. R. GOODY and M. J. S. BELTON, *Planet. Space Sci.* **15**, 247 (1967).
16. D. K. EDWARDS, L. K. GLASSEN, W. C. HAUSER and J. S. TUCHSCHER, *J. Heat Trans.* **86**, 219 (1967).
17. C. L. TIEN, Thermal Radiation Properties of Gases. *Advances in Heat Transfer*, Vol. 5. Academic Press, New York (1968).
18. M. VAN DYKE, *Perturbation Methods in Fluid Mechanics*. Academic Press, New York (1964).
19. R. D. CESS and S. N. TIWARI, *Appl. Scient. Res.* **19**, 439 (1968).
20. W. P. SCHIMMEL, J. L. NOVOTNY and F. A. OLSOFKA, Interferometric Study of Radiation-Conduction Interaction, *Proceedings of the Fourth International Heat Transfer Conference*, Paris-Versailles, Vol. III (1970).

21. S. I. RASOOL, J. S. HOGAN and R. W. STEWART, *J. Atmos. Sci.* **27**, 841 (1970).
22. J. S. HOGAN, R. W. STEWART, S. I. RASOOL and L. H. RUSSEL, *Radio Sci.* (in press).
23. J. T. HOUGHTON, *Quart. J. R. Met. Soc.* **89**, 319 (1963).
24. S. N. TIWARI and R. D. CESS, *JQSRT* **11**, 237 (1971).
25. C. BOYER and P. GUERIN, *Compt. Rend.* **263**, 253 (1966).
26. B. SMITH, *Science* **158**, 114 (1967).
27. A. DOLLFUS, Synthesis on Ultra-violet Survey of Clouds in Venus Atmosphere, *Atmospheres of Venus and Mars*. Gordon and Breach, New York (1968).
28. M. McELROY and D. STROBEL, *J. Geophys. Res.* **74**, 1118 (1969).
29. M. SHIMIZU, *Icarus* **10**, 11 (1969).
30. P. J. GIERASCH, *Icarus* **13**, 25 (1970).
31. T. GOLD and S. SOTER, *Icarus* **14**, 16 (1971).
32. G. FJELDBO, A. J. KLIJORE and V. R. ESHLEMAN, *Astronom. J.* **76**, 123 (1971).